Super-broadband continuum at UV-visible wavelengths generated by ultrashort laser-pulses in air

S. Skupin, and F. Lederer

Institute of Condensed Matter Theory and Solid State Optics, Friedrich-Schiller-Universität, 07743 Jena, Germany
+493641947173, +493641947177, stefan@pinet.uni-jena.de

L. Bergé

Département de Physique Théorique et Appliquée, CEA/DAM Ile de France, B.P. 12, 91680 Bruyères-le-Châtel, France

G. Méjean, J. Kasparian, J. Yu, S. Frey, E. Salmon, R. Ackermann, J.P. Wolf

Laboratoire de Spectrométrie Ionique et Moléculaire, Université Cl. Bernard Lyon 1, UMR-CNRS 5579, F-69622 Villeurbanne cedex, Lyon, France

Abstract: We report experimental and numerical results on supercontinuum generation at ultraviolet/visible wavelengths produced by the long-range propagation of infrared femtosecond laser pulses in air.

OCIS codes: (190.5530) Pulse propagation and solitons; (320.7110) Ultrafast nonlinear optics

While propagating in air, ultrashort laser pulses undergo filamentation [1] due to the dynamic interplay between Kerr focusing and self-induced plasma defocusing. Depending on the beam power, this subtle balance generates light filaments, which can develop over several hundreds of meters [2] and even kilometers in the vertical direction [3]. Associated with this property, the temporal variations experienced by the pulse produce a very broad spectral continuum, spanning from ultraviolet (UV) to infrared (IR) wavelengths. Coherence is preserved between the different spectral components, so that the broadened pulse is often referred to as a "white light laser" [4]. Most experimental and theoretical investigations using femtosecond Ti:Sa laser sources (800 nm) reported spectral broadening extending from 4.5 μm to an UV cut-off around 350 nm [5,6]. However, recent laboratory results demonstrated that another emission peak around 265 nm arises from an additional process: Third Harmonic Generation (THG) [7,8]. Over much longer scales, km-range propagation of TW laser pulses was found to enhance the spectrum intensity by two orders of magnitude in the IR domain [9]. Information on the UV regions of the spectra in this context is, however, missing. Here we report the first observation of a super-broadband continuum at UV-visible wavelengths with a cut-off as low as 230 nm, induced by the propagation of ultrashort laser pulses. This spectacular broadening, yielding the broadest coherent laser source ever observed, opens new trends in remote sensing of pollutants having strong UV absorption bands. The broadening is explained by the self-phase modulation of the fundamental pulse, which is amplified by the phase-locked third harmonics (TH) [7]. Moreover, direct numerical simulations show that THG behaves as a quintic saturation for the fundamental pulse, which enlarges the self-guiding length.

Two different experiments were performed. On the one hand, a Ti:Sa CPA laser system provided ~ 60 GW pulses (9 mJ, ~ 150 fs) centered at 810 nm. The 12 mm diameter beam freely propagated over 6.1 m and was focused with a $f = 5$ m convergent mirror, so as to produce a single filament at a distance of about 3.3 m from the mirror. The UV-visible part of the supercontinuum, reflected from the edge of a glass plate set very close to the filament, was measured with a photomultiplier tube attached to a monochromator, providing 7 nm spectral resolution. On the other hand, the Teramobile laser system [10] was arranged in a Light Detection and Ranging (Lidar) configuration [11]. It delivered 10-Hz rated, 5 TW pulses (70 fs, 350 mJ) centered at 800 nm. A beam with 10 cm diameter was sent vertically into the atmosphere. The Rayleigh-Mie scattering signals were inverted with standard algorithms [11]. Chirp and beam focusing produced pulse duration of 150 fs and 10 m focal length, which optimized white-light generation at long distances. Spectra were measured with 10 nm resolution from 230 nm to 600 nm.

The spectral evolution resulting from the first setup is shown in Figure 1(a). At short distances close to the nonlinear focus (filamentation onset), noted $z_c \simeq 3.3$ m, self-phase modulation (SPM) widely broadens the pump spectrum. At 1.26 m from this distance, a 20 nm THG band appears around 270 nm. This spectral enlargement is comparable with that detected in laboratory [8] over some tens of cm. About 2 m later, THG is depleted and a continuous UV-visible plateau appears, creating a hump in the 300-500 nm region. At further distances, this plateau holds its shape, far beyond the end of the filament. The same behavior is

observed over several hundreds of meters in the case of Lidar measurements [Fig. 1(b)]: At 105 m, a 50 nm broad THG band appears around 270 nm. From 135 m, the spectrum changes into an ultrabroad, continuous UV-visible plateau, which forms a hump in the wavelength domain 300 nm $\leq \lambda \leq$ 500 nm. This hump persists at longer distances, whereas UV components become more depleted. Figs. 1(a) and 1(b) exhibit the same spectral dynamics. The build-up in wavelengths, however, arises over longer scales in the Lidar configuration. Because multiple filaments develop in broad, high-power (TW) pulses, this difference can be attributed to a cumulative effect from all filaments in the Teramobile bundle.

Next, we numerically reproduced this spectral dynamics, using a parallel radial code that integrates the propagation equations coupling the slowly-varying envelopes of the fundamental wave ($\mathcal{E}_\omega$) with the TH one ($\mathcal{E}_{3\omega}$). These equations read

$$i\partial_z \mathcal{E}_j + i\alpha_j \partial_t \mathcal{E}_j + \beta_j \nabla_\perp^2 \mathcal{E}_j - \frac{k_j''}{2}\partial_t^2 \mathcal{E}_j - \delta_j \mathcal{E}_j + \mathcal{F}_j + \mathcal{P}_j = 0, \tag{1}$$

where $j = \omega, 3\omega$. In Eq. (1), z is the propagation variable, t is the time coordinate retarded with respect to the group velocity of the pump wave, $\nabla_\perp^2 = r^{-1}\partial_r r \partial_r$; $\alpha_{3\omega} = \Delta v^{-1}$, where $\Delta v = 0.44$ cm/fs is the group-velocity mismatch, $\alpha_\omega = 0$, $\beta_{3\omega} = \beta_\omega/3 = 1/6k_0$; $k_\omega'' = 0.2$ fs^2/cm and $k_{3\omega}'' = 1$ fs^2/cm are the coefficients for group-velocity dispersion (GVD) and $\delta_{3\omega} = \Delta k \equiv 3k(\omega) - k(3\omega) = -5$ cm $^{-1}$ is the wave vector mismatch ($\delta_\omega = 0$). The function $\mathcal{F}_j$ represents the optical nonlinearities:

$$\mathcal{F}_\omega = \frac{k_0 n_2^{(\omega)}}{2}|\mathcal{E}_\omega|^2\mathcal{E}_\omega + \frac{k_0 n_2^{(\omega)}}{2\tau_K}\int_{-\infty}^{t} \mathrm{e}^{-\frac{t-t'}{\tau_K}}|\mathcal{E}_\omega(t')|^2 dt \mathcal{E}_\omega + 2k_0 n_2^{(\omega)}|\mathcal{E}_{3\omega}|^2\mathcal{E}_\omega + k_0 n_2^{(\omega)}\mathcal{E}_\omega^{*2}\mathcal{E}_{3\omega} \tag{2a}$$

$$\mathcal{F}_{3\omega} = 3k_0 n_2^{(3\omega)}|\mathcal{E}_{3\omega}|^2\mathcal{E}_{3\omega} + 6k_0 n_2^{(\omega)}|\mathcal{E}_\omega|^2\mathcal{E}_{3\omega} + k_0 n_2^{(\omega)}\mathcal{E}_\omega^3. \tag{2b}$$

It involves self-, cross-phase modulations (SPM, XPM resp.) and Four-Wave Mixing (FWM) that drives THG. Here, $n_2^{(\omega)} = 4\times10^{-19}$ cm^2/W and $n_2^{(3\omega)} = 8\times10^{-19}$ cm^2/W are the respective Kerr coefficients. The function $\mathcal{P}_j$ describes the plasma gain and losses modeled as

$$\mathcal{P}_j = -\frac{\beta_j k_0^2}{\rho_c}\rho\mathcal{E}_j + i\frac{\sigma_j}{2}\rho\mathcal{E}_j + i\frac{\beta_j^{(K_j)}}{2}|\mathcal{E}_j|^{2K_j-2}\mathcal{E}_j \tag{3}$$

$$\partial_t \rho = \sum_{j=\omega,3\omega}(\rho_{\mathrm{nt}} - \rho)\sigma_{(K_j)}|\mathcal{E}_j|^{2K_j} + \frac{\sigma_j}{U_i}\rho|\mathcal{E}_j|^2, \tag{4}$$

where the number of photons are $K_\omega = 8$, $K_{3\omega} = 3$, K_j, the multiphoton ionization (MPI) rates $\sigma_{(8)} = 2.88\times10^{-99}$ s^{-1}cm^{16}/W^8, $\sigma_{(3)} = 1.9\times10^{-28}$ s^{-1}cm^6/W^3, the inverse bremsstrahlung cross-sections $\sigma_\omega = 5.44\times10^{-20}$ cm^2, $\sigma_{3\omega} = 6\times10^{-21}$ cm^2, and the multiphoton absorption (MPA) coefficients are $\beta_\omega^{(8)} = 3.1\times10^{-98}$ cm^{13}/W^7, $\beta_{3\omega}^{(3)} = 2.3\times10^{-27}$ cm^3/W^2. Only oxygen ionization with gap potential $U_i = 12.1$ eV is considered for a neutral medium with density $\rho_{\mathrm{nt}} = 5.4\times10^{18}$ cm^{-3}; $\rho_c = 1.8\times10^{21}$ cm^{-3} is the plasma critical density defined at 800 nm. Eqs. (1-4) are close to the model proposed in [7], apart from the Raman-delayed Kerr response undergone by the IR pulse ($\tau_K = 70$ fs) [6], avalanche ionization and minor changes in the nonlinearities.

With Eqs. (1-4) we simulated one filament starting from a Gaussian pulse with waist $w_0 = 0.5$ mm, FWHM duration of 150 fs ($= \sqrt{2\ln 2}t_p$) and power ratio $P_{\mathrm{in}}/P_{\mathrm{cr}} = 4$. Fig. 1(c) shows its spectral evolution at different distances after the nonlinear focus $z_c \simeq 0.4$ m. The plotted quantity is the normalized spectral intensity integrated in space. Self-focusing first induces SPM in the fundamental pulse. At $z = 1.37$ m, the TH component broadens in turn around 266 nm. During this process, the phase difference between the fundamental and TH waves remains locked at the value π. At $z > 3$ m, the spectrum is increased by about one decade at visible wavelengths, while UV components become more attenuated. Fig. 1(c) confirms that the hump below 500 nm is actually caused by THG (see dashed line). Spectral distortions similar to Fig. 1(a) develop over comparable distances shifted from the self-focus point, $\Delta z = z - z_c \simeq 1-3$ m. They agree with the experimental data, apart from oscillations created by interferences between different peaks appearing in the pulse profile. Such oscillations are smoothed in the experimental spectra, measured with a resolution of 7 nm and averaged over 128 shots. Both numerical and experimental results emphasize a built-up of UV-visible wavelengths. We explain this phenomenon by SPM-induced spectral broadening of both the IR and the UV component, which overlaps in this spectral domain. Moreover, we observed another mechanism

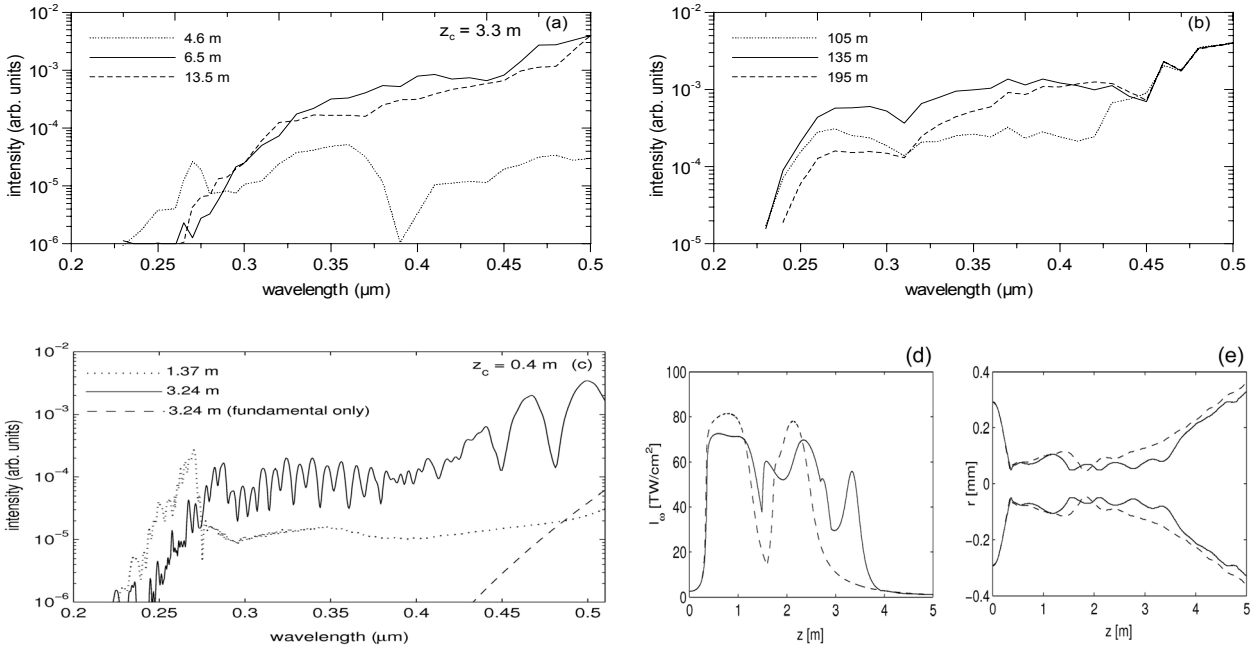

Fig. 1. Spectra in the wavelength domain 200 nm $\leq \lambda \leq$ 500 nm for different propagation distances. (a) Experimental data from laboratory measurements; (b) Spectra developing over 200 m measured by Lidar arrangement; (c) Spectra numerically computed from Eqs. (1) to (4). The dashed curve represents spectral broadening caused by the fundamental pulse only. In 1(a) and 1(c), z_c denotes the nonlinear focus (filament onset distance). Spectral intensity in the experiments is fixed to 4×10^{-3} times that in the fundamental at 500 nm [5], except for $z = 4.6$ m where its value is two decades below. Peak intensity (d) and Mean radius (e) (FWHM in the fluence distribution) of the IR pulse integrated numerically, with (solid) and without (dashed curves) THG.

which indirectly boosts SPM: Fig. 1(d) and 1(e) detail the peak intensities and mean radius of both coupled components (solid lines) and their counterpart when $\mathcal{E}_{3\omega} = 0$ (dashed lines), computed numerically. It is obvious that THG prolongates the filament range by ~ 1 m. SPM, as an intensity dependent process, takes place inside the filament only, and is therefore stronger with TH included. The enhancement of the filament range by TH generation is justified by the magnitude of the mismatch parameter $|\Delta k| = 5$ cm^{-1}, which is large compared with the nonlinear length scale $n_2 k_0 I_{\max} < 2.5$ cm^{-1}. In this situation, Eq. (1) for the TH component can be simplified by comparing the mismatch parameter with the FWM term responsible for THG (see [12]). This leads to the approximation $\mathcal{E}_{3\omega} \approx -(k_0 n_2/|\Delta k|)\mathcal{E}_\omega^3$, which acts as *a defocusing quintic nonlinearity* for the pump field equation. The TH pulse thus stabilizes the self-channeling process.

In conclusion, we have shown that the propagation of fs pulses in air is strongly influenced by the nonlinear dynamics of the third harmonic component. Coupling between the pump field and TH develops an important spectral broadening in the wavelength domain 200 nm $\leq \lambda \leq$ 500 nm, which favors supercontinuum generation. These properties were confirmed by numerical simulations, from which THG arised as a saturation mechanism for the pump wave. Experiments were performed in the framework of the Teramobile Project, funded jointly by CNRS and DFG.

References

1. A. Braun *et al.*, *Opt. Lett.* **20**, 73 (1995).
2. B. LaFontaine *et al.*, *Phys. Plasmas* **6**, 1615 (1999).
3. M. Rodriguez *et al.*, *Phys. Rev. E* **69**, 036607 (2004).
4. S.L. Chin, S. Petit, F. Borne, and K. Miyazaki, *Japan. Journal of Appl. Phys.* **38**, L126 (1999).
5. J. Kasparian *et al.*, *Opt. Lett.* **25**, 1397 (2000).
6. A. Couairon *et al.*, *J. Opt. Soc. Am. B* **19**, 1117 (2002).
7. N. Aközbek *et al.*, *Phys. Rev. Lett.* **89**, 143901 (2002).
8. H. Yang *et al.*, *Phys. Rev. E* **67**, 015401 (2003).
9. G. Méjean *et al.*, *Appl. Phys. B: Lasers and Optics* **77**, 357 (2003).
10. H. Wille *et al.*, *Eur. Phys. Jour. - Applied Physics* **20**, 183 (2002).
11. R. M. Measures, *"Laser remote sensing - Fundamentals and applications"*, Wiley Interscience, New York (1984).
12. A.V. Buryak, V.V. Steblina and R.A. Sammut, *Opt. Lett.* **24**, 1859 (1999).